OxLDL induces macrophage γ-GCS-HS protein expression: a role for oxLDL-associated lipid hydroperoxide in GSH synthesis

Lijiang Shen* and Alex Sevanian[1,*]

Department of Molecular Pharmacology and Toxicology,* School of Pharmacy, University of Southern California, 1985 Zonal Ave., Los Angeles, CA 90033

Abstract **Oxidized LDL (oxLDL) produced a rapid depletion of intracellular glutathione (GSH) followed by an adaptive increase in J774 A.1 macrophages. OxLDL also induced a transient increase in the levels of γ-glutamylcysteine synthetase heavy subunit (γ-GCS-HS), representing the catalytic subunit of the rate-limiting enzyme for de novo GSH synthesis. The induction took place within 3 h, with maximum levels observed by 10 h of treatment. Pretreatment of oxLDL with ebselen inhibited GSH depletion and attenuated the γ-GCS-HS induction. OxLDL-associated lipid hydroperoxides and their decomposition product aldehydes are two major components thought to account for GSH depletion in macrophages. Ebselen pretreatment had only a minor effect on malondialdehyde levels, whereas peroxide content was essentially abolished, suggesting that oxLDL-associated hydroperoxides may mediate both GSH depletion and γ-GCS-HS induction. Acetylated LDL (AcLDL) also caused a moderate induction of γ-GCS-HS protein along with a 30% transient increase in GSH by 3–6 h, suggesting a minor involvement of scavenger receptor-mediated signaling of GSH synthesis. However, the level of γ-GCS induction by AcLDL was insufficient to cause a sustained increase in GSH. Macrophages with higher glutathione peroxidase (GPx) activity experienced a more rapid and extensive depletion of GSH when treated with oxLDL under similar conditions, along with greater resistance to oxLDL- or peroxide-induced cytotoxicity. We conclude that oxLDL-associated peroxides are primarily responsible for GSH depletion, creating an oxidizing environment required for γ-GCS induction and compensatory GSH synthesis. This is facilitated in cells expressing high GPx activity through a rapid depletion of GSH in the face of a peroxide challenge.**—Shen, L., and A. Sevanian. **OxLDL induces macrophage γ-GCS-HS protein expression: a role for oxLDL-associated lipid hydroperoxide in GSH synthesis.** ***J. Lipid Res.*** **2001.** 42: **813–823.**

Supplementary key words oxidized low density lipoprotein • γ-glutamylcysteine synthetase • reactive oxygen species

Oxidized low density lipoprotein (oxLDL) is believed to play an important role in the pathogenesis of atherosclerosis (1). There is evidence that oxidation of LDL occurs in the arterial wall, and a variety of vascular cells, including monocyte-macrophages, can oxidize LDL in culture (2). Several mechanisms have been proposed for macrophage-mediated LDL oxidation, including cellular 15-lipoxygenase (3), NADPH oxidase (4), myeloperoxidase (5), and reactive nitrogen species (6). Oxidation of LDL-associated lipids and subsequent decomposition of lipid peroxidation products result in the modification of lysine residues of apolipoprotein B, leading to recognition by scavenger receptors on arterial macrophages. Unregulated uptake of oxLDL by macrophages contributes to foam cell and fatty streak formation. The class A scavenger receptor (7) and CD36 (8) are considered as major oxLDL receptors in monocyte-derived macrophages. Other receptors such as the class B type I scavenger receptor, macrosialin/CD68, and lectin-like oxLDL receptor 1 (LOX-1) have also been reported to bind oxLDL (9). Because the macrophage is the major cell type that sequesters oxLDL, it can likely be subjected to severe oxidative stress.

Glutathione (L-γ-glutamyl-L-cysteinyl-glycine, GSH) is the most abundant antioxidant in cells, and plays a major role in cellular defense against oxidative stress. GSH can directly scavenge free radicals (10) or act as a substrate for glutathione peroxidase(s) (GPx) and glutathione-*S*-transferase during the detoxification of hydrogen peroxide (H_2O_2), lipid hydroperoxides (11), and electrophilic compounds (12). GSH is synthesized in two sequential adenosine 5′-triphosphate (ATP)-dependent enzymatic reactions that are catalyzed by γ-glutamylcysteine synthetase (γ-GCS) and glutathione synthetase (13). Several factors control

Abbreviations: AP-1, activator protein 1; γ-GCS, γ-glutamylcysteine synthetase; γ-GGA, γ-glutamyl-glutamic acid; GPx, glutathione peroxidase; GSH, glutathione; GSSG, glutathione disulfide; LOOH, lipid hydroperoxides; oxLDL, oxidized low density lipoprotein; ROS, reactive oxygen species.

[1] To whom correspondence should be addressed.
e-mail: asevan@hsc.usc.edu

the rate of de novo GSH synthesis, the first of which is the rate-limiting enzyme γ-GCS, bearing a catalytic heavy subunit (γ-GCS-HS, M_r 73,000) and a regulatory light subunit (γ-GCS-LS, M_r 31,000). The second factor is the availability of cysteine, which is mainly derived from degradation of circulating GSH by γ-glutamyl transpeptidase (GGT) and dipeptidase (14). Another factor involves feedback inhibition of γ-GCS activity by GSH, in which approximately 80% of γ-GCS is inactive when GSH is present at the normal concentrations for a given cell type (15).

An initial acute decrease in GSH during exposure to sublethal doses of *tert*-butyl hydroperoxide (*t*-BuOOH), H_2O_2, or diamide was followed by an overproduction of GSH content (16), which may be due at least in part to the relief in the feedback inhibition of γ-GCS and the induction of enzyme. Other oxidants have been reported to cause γ-GCS activation without an initial significant depletion in GSH (17, 18). This could be explained by the relative flux between glutathione reductase (GRD)-mediated reduction of glutathione disulfide (GSSG) to GSH, and GPx- and/or GST-mediated oxidation and conjugation reactions at the expense of GSH. Like these hydroperoxides, oxLDL has been shown to cause an initial decrease followed by an adaptive increase of GSH in macrophages (19) and human vascular endothelial cells (20). Although the molecular mechanism by which this takes place is unclear, the initial depletion of GSH might be due to the detoxification of oxLDL containing lipid hydroperoxides (LOOH) or aldehydes. The formation of GSSG or GSH conjugates and their exportation from the cells lead to a net loss of GSH (21). Although GSH can be partially recovered by the action of GRD after an oxidative stress, it appears to be of minor importance compared with GSH production via de novo synthesis. The GSH adaptive increase is considered as cellular defense against oxidative stress. Increased expression of γ-GCS-HS mRNA and GSH have been found after oxLDL treatment (20), suggesting de novo synthesis of GSH. Moreover, the induction of γ-GCS is mediated by activation of activator protein 1 (AP-1). AP-1 is a heterodimer composed of the c-Fos and c-Jun proteins, or a homodimer of c-Jun proteins. AP-1 controls the expression of many genes, and activates these genes by binding to 12-*O*-tetradecanoylphorbol 13-acetate response elements (TRE) (22).

In this study, we investigated major oxLDL-associated factors underlying GSH depletion and repletion in relation to oxLDL-induced oxidative stress in macrophages. Our findings show that oxLDL peroxide content is a major determining factor for the depletion and compensatory repletion of GSH through the enhanced expression of γ-GCS.

MATERIALS AND METHODS

Materials

J774A.1 macrophage cell line was purchased from the American Type Culture Collection (ATCC, Manassas, VA). Sodium selenite, GSH, GSSG, fucoidin, GSH reductase, NADPH, 3-(4,5-dimethylthiazol-2-yl)-2,5-diphenyl-tetrazolium bromide (MTT), *t*-BuOOH, diethylenetriaminepentaacetic acid free acid (DTPA), 2,4-dinitrofluorobenzene, and 2′,7′-dichlorofluorescein diacetate (DCFH-DA) were obtained from Sigma (St. Louis, MO). γ-Glutamyl-glutamic acid (γ-GGA) was from Bachem Bioscience (Torrance, CA). 1,1′-Dioctadecyl-3,3,3′,3′-tetramethylindocarbocyanine perchlorate (DiI) was from Molecular Probes (Eugene, OR).

Cell culture

J774A.1 macrophages were maintained in Dulbecco's modified Eagle's medium (DMEM) supplemented with 10% (v/v) fetal bovine serum (FBS) (Omega Scientific, CA) and gentamicin (0.05 mg/ml) (Omega Scientific), at 37°C in a humidified incubator (5% CO_2, 95% air). Experiments were performed when cells were about 90% confluent.

Isolation of LDL from human plasma

Human LDL (d 1.019–1.063 g/ml) was prepared by ultracentrifugation, using a Beckman (Fullerton, CA) L8-55 ultracentrifuge equipped with SW-41 rotors as described previously (23). The LDL fraction was dialyzed and concentrated with a centrifugal filter device (Millipore, Bedford, MA) with a molecular weight cutoff of 30,000. LDL at 1 mg of protein per ml of phosphate-buffered saline (PBS) containing 100 μM ethylenediaminetetraacetic acid (EDTA) was sterilized by filtration through a 0.2-μm pore size syringe filter (Corning, Corning, NY) and stored at 4°C until used for various experiments. Protein concentration was measured by the Bio-Rad (Hercules, CA) protein assay reagent, using bovine serum albumin as a standard.

LDL modification

Human LDL was diluted to 0.2 mg of LDL protein per ml and incubated with 10 μM $CuSO_4$ for 20 h at 37°C. Oxidation was terminated by adding 100 μM EDTA and cooling. LDL was dialyzed and reconcentrated to 1-mg protein per ml, sterilized, and stored at 4°C in PBS containing 100 μM EDTA. Acetylated LDL (AcLDL) was prepared by chemical modification of LDL with acetic anhydride as described by Basu et al. (24). LOOH levels for unmodified LDL (nLDL), AcLDL, and oxLDL were 25.9 ± 12.8, 23.7 ± 2.3, and 1,528 ± 66 nmol/mg LDL protein, respectively.

LDL^- separation

LDL^- (electronegatively charged LDL) was separated from human total plasma LDL by ion-exchange high performance liquid chromatography (HPLC) (Bio-Rad) with a UNO Q1 column (Bio-Rad) (23). After HPLC, the LDL^- fraction was purified and salts were removed by centrifugal dialysis, using a 30,000 molecular weight cutoff filter. The samples were then diluted in PBS and added to cultured cells. The LOOH levels for LDL^- were about 700–800 nmol/mg LDL protein.

Measurement of H_2O_2 metabolism

H_2O_2 in cell culture medium was measured with a biological oxygen monitor (Yellow Springs Instrument, Yellow Springs, OH) after the addition of excess catalase (25). J774 macrophages ($1–2 \times 10^7$) were plated in a 100-mm dish with 20 ml of RPMI medium 1640 (Life Technologies, Rockville, MD). An initial concentration of 100 μM H_2O_2 was added to medium and samples were taken every 5 min to measure the remaining H_2O_2 concentration. A calibration curve was made with H_2O_2 reagent for each experiment.

Lipid peroxide measurement

LOOH levels in LDL were determined by the modified method of Auerbach, Kiely, and Cornicelli (26). Samples were added to a mixed solution containing leukomethylene blue (LMB) and hemoglobin for 1 h. Oxidation of LMB to methylene

blue was monitored at 650 nm, using a microplate reader (Cambridge Technology, Cambridge, MA). *t*-BuOOH was used as calibration standard.

Thiobarbituric acid reaction (TBAR) measurement

The TBAR assay is a modified method of Buege and Aust (27). Samples (0.5 ml) were mixed thoroughly with 1 ml of a solution containing 15% (w/v) trichloroacetic acid, 0.375% (w/v) TBA, and 0.25 N hydrochloric acid, and heated for 15 min. After cooling, the flocculent precipitates were removed by centrifugation. The absorbance of the sample was determined at 535 nm against a blank containing all reagents except the LDL samples. The malondialdehyde (MDA) equivalent concentration was calculated with an extinction coefficient of $1.56 \times 10^5\ M^{-1}\ cm^{-1}$.

In vitro GSH depletion assay

The in vitro GSH depletion assay is modified from the method of Roveri, Maiorino, and Ursini (28). Cells were lysed in PBS by ultrasonication and centrifuged at 2,000 rpm for 5 min. NADPH depletion rates were measured at 340 nm for 8 min, using a Beckman DU-650 spectrophotometer, in a reaction mixture containing 0.2 mM NADPH, 0.1% Triton X-100, 0.1 M Tris buffer containing 5 mM EDTA, 1 unit of GSH reductase, 3 mM GSH, and cell lysate (derived from 100 μg of cell protein) to which 200 μM *t*-BuOOH was added as a substrate. Basal rates of depletion were obtained with all reagents except cell lysate. GSH depletion rates are calculated by assuming that 1 mol of NADPH depletion is equivalent to 2 mol of GSH.

LDL uptake by macrophages

Measurement of LDL uptake by J774 cells was accomplished with fluorescently labeled LDL, referred to as DiI-LDL. DiI-LDL was prepared by incubating LDL (500 μg/ml) with DiI in dimethyl sulfoxide to reach a final concentration of 50 ng of DiI per μg LDL. Cells ($2–3 \times 10^5$) were then incubated with 10 μg of DiI-LDL per ml at 37°C for 3 h. The cell monolayer was washed twice with PBS, followed by addition of 1.2 ml of isopropyl alcohol. Plates were shaken gently at room temperature in the dark for 30 min. The sample extracts were measured in a fluorometer (Hitachi, San Jose, CA; excitation, 523 nm; emission, 563 nm). The amount of uptake was corrected on the basis of cell protein content.

Enzyme assays

GPx activity was determined by spectrophotometrically monitoring the oxidation of NADPH at 340 nm. One unit of activity was defined as the amount of enzyme catalyzing the oxidation of 1 nmol of NADPH per min. Assay mixtures (1 ml) contained 3 mM GSH, 0.2 mM NADPH, 1 unit of GRD, 0.5% Triton X-100, and 100 μg of cell protein in 100 mM Tris buffer containing 5 mM EDTA (pH 7.4). *t*-BuOOH was used as a substrate. Because *t*-BuOOH is a common substrate for both cytosolic glutathione peroxidase (cGPx) and phospholipid glutathione peroxidase (PHGPx), this assay represents total GPx activity.

GRD activity was determined by monitoring the decrease in absorbance at 340 nm during the reduction of GSSG by NADPH (29). Reaction mixtures contained 0.1 M potassium phosphate buffer (pH 7.6), 1 mM GSSG, 0.1 mM NADPH, and 100 μg of cell protein.

Catalase activity was determined by monitoring H_2O_2 consumption at 240 nm. Assay mixtures (0.5 ml) included 300 μl of 0.05 M potassium phosphate buffer containing 1 mM DTPA, 100 μg of cell protein, and 100 μl of 100 mM H_2O_2. Sample absorbance was monitored every 0.2 s for 2 min. Results were plotted semilogarithmically against time ($\varepsilon_{240\ nm} = 43.6\ M^{-1}\ cm^{-1}$). Catalase activity was determined from the slope of the plot divided by cell protein ($k' = s^{-1}\ mg^{-1}$).

Measurement of intracellular GSH

Intracellular GSH and GSSG content were determined by HPLC according to the method of Fariss and Reed (30). Briefly, cell samples after various treatments were washed twice with ice-cold PBS and collected in 1 ml of 10% perchloric acid containing 2 mM EDTA and 7.5 nmol of γ-GGA (Bachem Bioscience) as an internal standard. After centrifugation, supernatants were collected, derivatized with 2,4-dinitrofluorobenzene, and analyzed for GSH, GSSG, and γ-GGA content by HPLC.

Western-blot analysis

J774A.1 macrophages were washed twice with Dulbecco's PBS, scraped, and collected by low speed centrifugation. The cell pellet was lysed in 150 μl of 0.3% sodium dodecyl sulfate-50 mM Tris (pH 8.0)-1% 2-mercaptoethanol and then treated with 10 μl of RNase/DNase solution [DNase (1 mg/ml), RNase A (0.5 mg/ml), 500 mM Tris (pH 6.8), and 50 mM $MgCl_2$] for 1 min. The samples were mixed with 5× Laemmli sample loading buffer (4:1), heated for 2 min at 100°C, and separated electrophoretically on a 12% polyacrylamide gel (Bio-Rad). Proteins were transferred to Immobilon P membranes (Millipore) at 100 V for 1 h. The membrane was blotted with 5% nonfat dry milk in Tris-buffered saline with Tween 20 for 1–2 h. Rabbit anti-mouse cGPx or PHGPx antibody (provided by Dr. F. Ursini, Department of Biological Chemistry, University of Padua, Italy) was diluted 1:1,000 and incubated with membranes for 2 h at 37°C. Rabbit anti-rat γ-GCS-HS antibody (provided by Dr. H. Forman, Department of Environmental Health Sciences, School of Public Health, University of Alabama at Birmingham, Birmingham, AL) was diluted 1:5,000 and incubated with membranes overnight at 4°C. The guidelines provided in the enhanced chemiluminescence Western blotting kit for chemiluminescence detection with Hyperfilm were followed. Protein bands were quantified by densitometry.

MTT cytotoxicity assay

Cell viability was determined spectrophotometrically by measuring mitochondrial dehydrogenase activity (31). Briefly, cells were plated on a 48-well dish (Corning) and treated with 200 μM H_2O_2. After treatment, stock MTT solution (5 mg/ml) was added to each well at 10% of culture medium volume, and incubated for 2 h at 37°C. After the incubation, the original medium was removed and dissolved in isopropanol for 30 min. Absorbance was measured at 570 nm, using a microplate reader. The extent of cytotoxicity was determined from the number of surviving cells as calculated from the amount of formazan produced in control and treated cells.

Statistical analysis

Data are expressed as means ± SE unless indicated otherwise and evaluated by Student's *t*-test. For all analyses, $P < 0.05$ is considered significant. The numbers of samples used in each experiment are indicated under Results or in the figure legends.

RESULTS

Changes in GSH levels after oxLDL treatment

To study the effects of oxLDL on intracellular GSH, we measured the changes in GSH levels over a 24-h period in J774A.1 macrophages treated with a 200-μg/ml concentration of oxLDL, LDL^-, AcLDL, and nLDL. A marked decrease in GSH was observed within 3 h after oxLDL treatment, followed by a recovery to basal levels at 6 h and an adaptive increase by 24 h (**Fig. 1**). GSH continued to increase to 30 h of incubation and then gradually de-

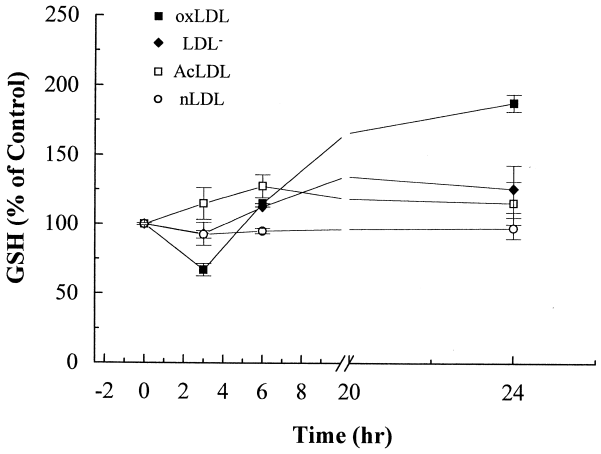

Fig. 1. Time course of macrophage intracellular GSH changes following low density lipoprotein (LDL) treatments. J774A.1 macrophages (2×10^6 cells/well) were treated with 200 μg/ml oxLDL (solid squares), LDL^- (solid diamonds), AcLDL (open squares), and nLDL (open circles) for up to 24 h in 10% fetal bovine serum-Dulbecco's modified Eagle's medium (FBS-DMEM). Intracellular GSH levels were determined as described in Materials and Methods. The GSH content is expressed as a percentage relative to untreated controls. Data represent means ± SE (%) for at least three independent experiments.

creased to basal levels (data not shown). Mildly oxidized LDL (LDL^-) (23), which is not a ligand for the scavenger receptor (32), produced a small and nonsignificant initial decrease and subsequent increase in GSH levels. In contrast, nLDL had no effect on intracellular GSH levels. AcLDL caused no GSH depletion but elicited a transient 30% increase between 3 and 6 h. Both the initial depletion and adaptive increase in GSH were oxLDL dose dependent as shown in **Fig. 2**. No severe toxicity has been found at this level of oxLDL treatment (data not shown), indicating the decrease in GSH was not due to compromised cell metabolism. Together these data suggest that only oxidatively modified LDL is able to induce significant GSH depletion and an adaptive increase in macrophages.

OxLDL-induced GSH depletion is primarily due to LOOH

LDL lipid peroxidation leads to formation of LOOH and their degradation products, aldehydes, such as MDA. We considered that these two components might be primarily responsible for GSH depletion. To determine the contribution of these components in oxLDL-induced GSH changes, ebselen [2-phenyl-1,2-benzisoselenazol-3(2*H*)-one] was used to reduce peroxides in oxLDL. Ebselen, an organic seleno compound with GPx-like activity (33), has been shown to effectively reduce oxLDL-associated peroxides. Pretreatment of oxLDL with 50 μM ebselen and 3 mM GSH for up to 30 min reduced the peroxide (LOOH) content by greater than 90%, with only a minor effect on MDA levels (**Fig. 3A**). Ebselen treatment did not affect oxLDL uptake by macrophages as shown in Fig. 3B, and uptake of a similar amount of DiI-oxLDL was found for ebselen-treated and untreated oxLDL by macrophages.

Ebselen-treated oxLDL at a dose of up to 200 μg/ml caused neither the initial GSH depletion nor the subsequent adaptive GSH increase (**Fig. 4A**). These effects were not likely due to residual ebselen activity in the oxLDL, because the GPx-like activity of potentially contaminating ebselen was about 10 nmol/min/mg LDL, less than 10% of the GPx level in macrophages under normal culture conditions. LDL isolated from various plasma pools was oxidized by Cu^{2+}, using the same procedure, and LOOH levels in oxLDL ranged from 1,300 to ~2,800 nmol/mg LDL protein (with a median value of ~1,600 nmol). By contrast there was only 23.7 ± 2.3 nmol of LOOH per mg LDL protein in AcLDL. The oxLDL- and AcLDL-induced GSH changes were plotted against the LOOH concentrations in the various preparations that were added to the cells at an equivalent oxLDL or AcLDL concentration of 200 μg/ml. A strong correlation ($R = -0.869$) was found between GSH depletion and the oxLDL-associated LOOH concentration (Fig. 4B). This suggests that LOOH-induced GSH oxidation may be responsible for GSH depletion. However, a relatively weak correlation ($R = 0.427$) was found between the GSH adaptive increase and LOOH levels (data not shown), suggesting that more complex mechanisms may be involved in peroxide-induced GSH redox changes and GSH de novo synthesis. Together these findings suggest that the uptake of oxLDL-associated LOOH induces the macrophage GSH depletion that could in part trigger the de novo synthesis.

Induction of γ-GCS-HS protein by oxLDL

Intracellular GSH levels are mainly regulated by the activity of rate-limiting enzyme γ-GCS (34). Western analysis

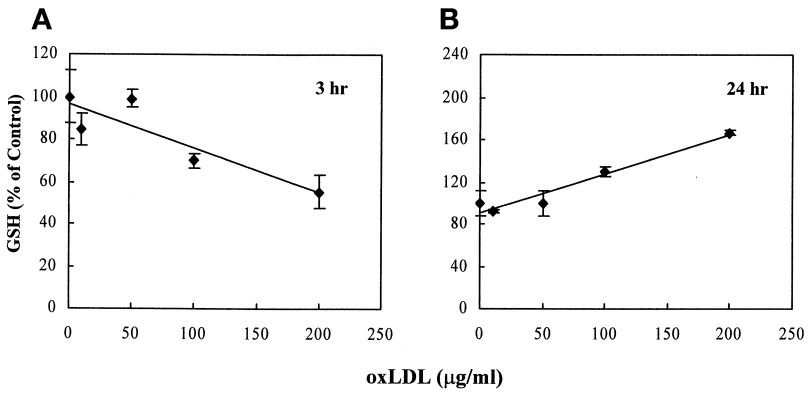

Fig. 2. Dose-dependent effects of oxLDL on GSH depletion and adaptive increase. J774A.1 macrophages (2×10^6 cells per well) were treated with oxLDL at 0, 10, 50, 100, and 200 μg/ml for 3 or 24 h. A: OxLDL-induced GSH decrease at 3 h. B: OxLDL-induced GSH increase at 24 h. The GSH content is expressed as the mean ± SE (%) of untreated controls for three independent analyses, with duplicate measurements at each time point.

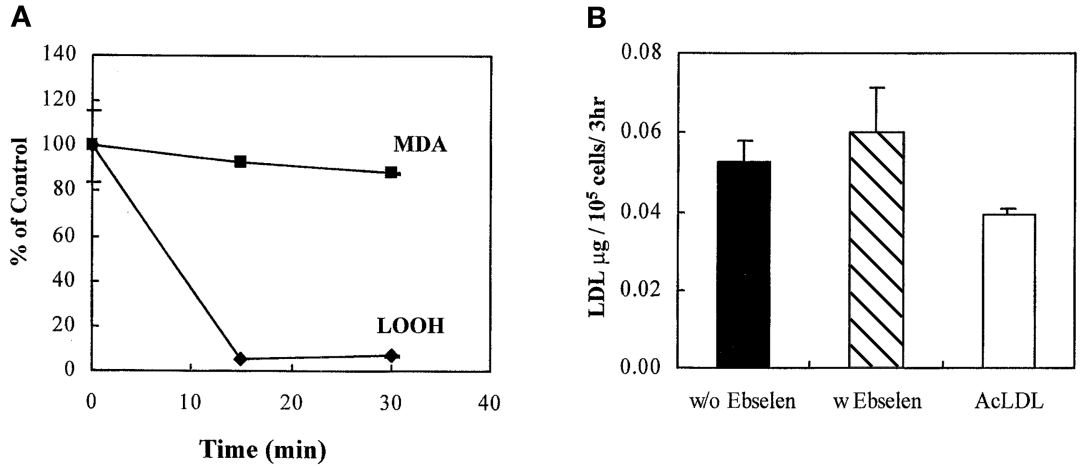

Fig. 3. The effects of ebselen pretreatment on oxLDL and uptake of oxLDL by macrophages. A: OxLDL was pretreated with 50 μM ebselen plus 3 mM GSH for 30 min at 37°C, and then briefly washed with phosphate-buffered saline (PBS), using a microfilter to remove excess ebselen and GSH. The LOOH and MDA levels were determined as described in Materials and Methods. LOOH levels in nLDL and oxLDL were 25.9 ± 12.8 and 1,528 ± 66 nmol/mg LDL protein, respectively, and malondialdehyde (MDA) levels in nLDL and oxLDL were 1.3 ± 0.12 and 12.5 ± 3.6 nmol/mg LDL protein, respectively. Data represent means ± SE (%) of three independent experiments. B: DiI-LDL was prepared by incubating oxLDL (500 μg/ml) with DiI to reach a final concentration of 50 ng of DiI per μg LDL. Cells ($2–3 \times 10^5$) were then incubated with 10 μg of DiI-LDL per ml at 37°C for 3 h as described in Materials and Methods. LDL uptake is expressed as micrograms of LDL protein per 10^5 cells in 3 h. AcLDL was used as a positive control for scavenger receptor-mediated LDL uptake. Data represent means ± SE for two independent experiments, with triplicate measurements for each sample.

of γ-GCS-HS protein expression was performed to determine whether the GSH increases produced by oxLDL were due to γ-GCS induction. When cells were treated with oxLDL at 200 μg/ml, a transient increase in γ-GCS-HS protein was observed as early as 3 h, with a maximum 4- to 5-fold increase by 10 h followed by a sustained 2-fold protein induction at 24-h post-treatment (**Fig. 5A**). The induction of γ-GCS-HS enzyme appears to account for the oxLDL-induced adaptive increase in GSH after its initial depletion as shown in Fig. 1. In contrast, nLDL had only a minor effect on γ-GCS-HS expression. AcLDL, and ebselen-pretreated oxLDL, also induced an increase in γ-GCS-HS levels, with similar but truncated patterns of expression over time that were approximately 55% and 35% less, respectively,

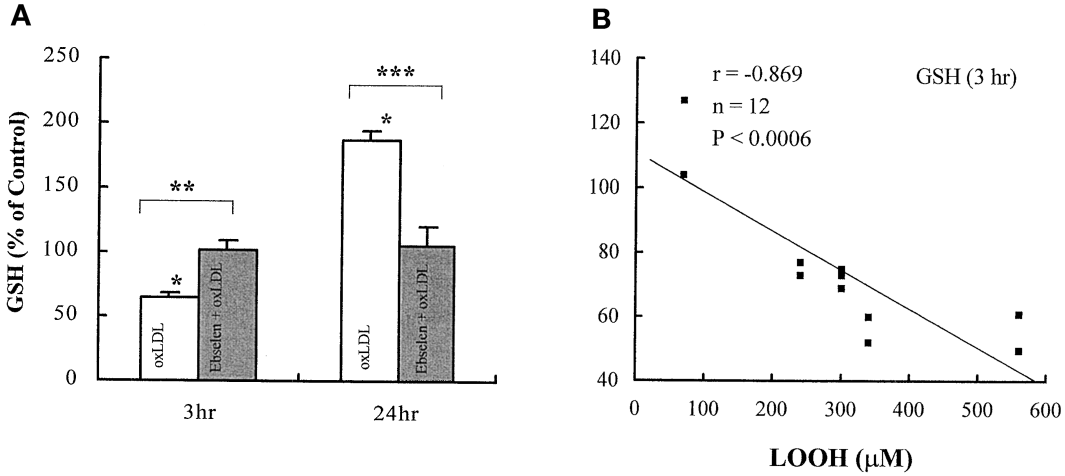

Fig. 4. Effects of ebselen-treated oxLDL on macrophage GSH status and the correlation between oxLDL LOOH content and GSH depletion. A: Effects of ebselen-treated oxLDL on macrophage GSH status. J774A.1 macrophages ($2–3 \times 10^6$/well) were treated with oxLDL at 200 μg/ml (n = 4) (white columns) and ebselen-pretreated oxLDL (n = 5) (gray columns) for 3 or 24 h. Data are expressed as means ± SE (%) for three independent experiments. The basal GSH level is considered as 100%. * $P < 0.05$, compared with 0-h untreated control; ** $P < 0.05$, compared with 3-h oxLDL treatment; *** $P < 0.05$, compared with 24-h oxLDL treatment. B: Correlation between oxLDL LOOH content and GSH depletion. LDL isolated from various plasma pools was modified by the same procedure in more than five separate experiments. The LOOH content for oxLDL ranges from 1,300 to ~2,800 nmol/mg LDL protein, with a median value of ~1,600 nmol/mg LDL protein, whereas the LOOH content for AcLDL was only 23.7 ± 2.3 nmol/mg LDL protein. GSH depletion (% of nontreated control) was plotted against LOOH concentrations that were equivalent to an oxLDL or AcLDL concentration of 200 μg/ml. Data are expressed as the mean of duplicate measurements for each sample.

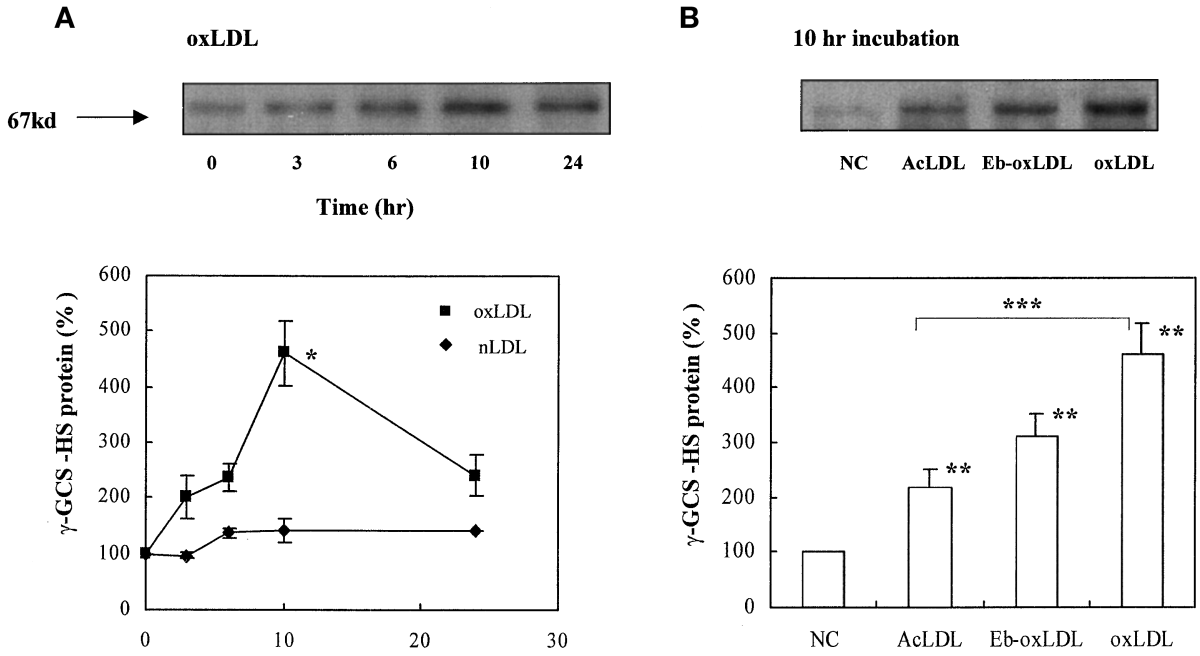

Fig. 5. OxLDL-induced γ-GCS-HS protein expression. J774A.1 macrophages ($2–3 \times 10^6$/well) were treated with a 200-μg/ml concentration of nLDL, AcLDL, oxLDL, and ebselen-pretreated oxLDL (Eb-oxLDL) for the incubation periods indicated. γ-GCS-HS protein levels were determined by Western-blot analysis, using anti-rat γ-GCS-HS antibody. Data are expressed as a percentage relative to nontreated control (NC). A: Induction of γ-GCS-HS protein by oxLDL and nLDL. Macrophages were treated with oxLDL (solid squares), nLDL (solid diamonds) for 0, 3, 6, 10, and 24 h. The images were quantified by densitometry. * Significantly different from nLDL at 10 h ($P < 0.05$). B: γ-GCS-HS protein expression at 10 h of incubation. AcLDL (n = 3), oxLDL (n = 4), and Eb-oxLDL (n = 4). ** Significantly different from NC ($P < 0.05$); *** significantly different from AcLDL ($P < 0.05$).

than oxLDL treatment at 10 h (Fig. 5B). These data suggest a peroxide-mediated de novo GSH synthesis via induction of γ-GCS after exposure to oxLDL. However, other alternative pathways such as the scavenger receptor-mediated signaling events may also contribute to enzyme induction.

OxLDL-induced macrophage ROS production

It is well known that γ-GCS activity and transcription can be affected by a variety of factors that produce reactive oxygen species (ROS) (35). To determine whether oxLDL-induced ROS production in J774 macrophages corresponded to the induction of GSH synthesis, cells were treated with a 200-μg/ml concentration of nLDL, AcLDL, and oxLDL for 3 h, and then labeled with 100 μM DCFH-DA for another 30 min, followed by measurement of DCF absorbance at 502 nm. nLDL, AcLDL, and oxLDL treatment induced DCF production by 106 ± 5.2%, 125 ± 9.9%, and 136 ± 13.5%, respectively, relative to the spontaneous rate of DCF oxidation in cells as shown in **Fig. 6**. This suggests that ROS generation is associated with LDL-scavenger receptor binding and may be involved in macrophage γ-GCS expression.

Characterization of antioxidant enzyme activities in selenium-supplemented cells

A primary function of GPx is to reduce peroxides and prevent propagation of radical chain reactions during lipid peroxidation. GPx detoxifies peroxides at the expense of GSH, and thus the metabolism of peroxides can affect GSH levels through the catalytic action of selenoperoxidases. We investigated the effects of oxLDL and peroxides in cells that were supplemented with selenium [Se (+) cells].

Na_2SeO_3 (100 nM supplementation) increased macrophage GPx activity, which reached maximal levels by 6–7 days (data not shown). Se (+) cells exhibited a 6-fold increase in total GPx activity, which corresponded to a 4-fold

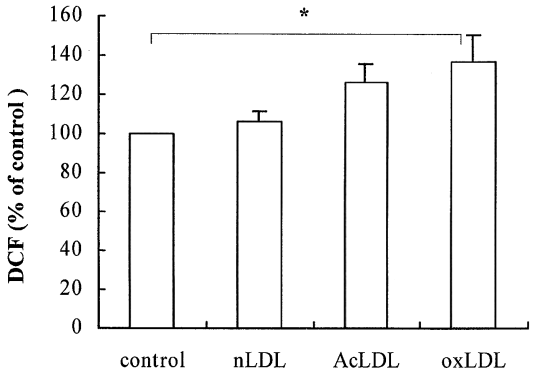

Fig. 6. LDL-induced ROS production in J774 macrophages. J774A.1 macrophages were plated in a 24-well dish ($2–3 \times 10^5$/well) and treated with a 200-μg/ml concentration of nLDL, AcLDL, and oxLDL for 3 h, and then labeled with DCFH-DA for 30 min as described in Materials and Methods. The absorbance of dichlorofluorescein (DCF) at 502 nm was measured spectrophotometrically, and the distribution of DCF in cells was expressed as a percentage relative to control. * Significantly different from control ($P < 0.05$).

TABLE 1. Effects of selenium supplementation on antioxidant enzyme activities, protein content, and GSH levels in J774A.1 macrophages

Cell Type	Enzyme Activity			Protein Content		
	GPx	GRD	CAT	cGPx	PHGPx	GSH
	U/mg cell protein		*1 × mg^{-1} protein × s^{-1}*	*relative intensity*		*nmol/mg cell protein*
Control cells	116 ± 42	6.1 ± 0.6	0.059 ± 0.003	9.4 ± 3.1	10.6 ± 2.4	26.7 ± 2.4
Se (+) cells	656 ± 16	6.4 ± 0.1	0.054 ± 0.012	30 ± 3.5	17.3 ± 1.3	28.5 ± 2.5

J774A.1 macrophages were supplemented with 100 nM Na_2SeO_3 in 10% FBS plus DMEM for 1 week. Data represent the mean ± SE of three or more independent experiments. GPx, total GPx activity; GRD, glutathione reductase; CAT, catalase; cGPx, cystolic GPx; PHGPx, phospholipid GPx.

increase in cGPx protein and ~2-fold increase in PHGPx protein, as quantified in **Table 1**. Other antioxidant enzyme activities such as GRD and catalase remained unchanged. Likewise, the intracellular GSH content was unaffected under these conditions.

To characterize the detoxification capacity in Se (+) cells with higher GPx activity, we measured GSH consumption after peroxide addition to cell lysates. Se-supplemented cells were found to be more resistant to peroxide-induced challenge than control cells. The GSH consumption rate for Se (+) cells was about five times faster than that of control cells after addition of 200 μM *t*-BuOOH (**Fig. 7A**). The faster GSH depletion rates in Se (+) cells were also associated with 20% greater peroxide (H_2O_2) consumption rates compared with control cells (Fig. 7B). Because H_2O_2 is a substrate for both catalase and GPx, a more substantial difference may be expected for peroxide consumption if substrate were limited specifically to GPx. Finally, we compared the cytotoxicity of H_2O_2 in Se (+) cells versus control cells. Macrophages were treated with 200 μM H_2O_2, and cell viability was determined by the MTT assay (Fig. 7C). The extent of resistance to oxidative stress was directly correlated with the GPx activity and the peroxide metabolism rate of the cells.

OxLDL-induced GSH and γ-GCS-HS changes in Se (+) cells

To determine whether Se (+) cells that display an enhanced capacity to eliminate H_2O_2 also had a greater response in terms of oxLDL-induced GSH depletion and repletion, we treated Se (+) cells with oxLDL (200 μg/ml) for up to 24 h. OxLDL treatment caused a more rapid initial decrease but a less extensive adaptive increase of GSH levels in Se (+) cells. The rapid depletion of GSH after 3 h of treatment of Se (+) cells with oxLDL was accompanied by a 2-fold increase in GSSG/GSH ratios, whereas only a 30% increase was found in control cells (**Fig. 8A**). The increase in GSSG/GSH ratio was positively correlated with cellular GPx levels ($R = 0.78$) (data not shown). Moreover, oxLDL induced a more rapid but moderate increase in γ-GCS-HS protein levels in Se (+) cells, achieving maximum levels that were about 25% lower than that found in control cells (Fig. 8B). Taken together, these findings show that Se (+) cells bearing higher GPx activities indeed detoxify more peroxides and utilize GSH more rapidly, but this does not determine the extent of peroxide-mediated γ-GCS-HS protein induction and GSH increase.

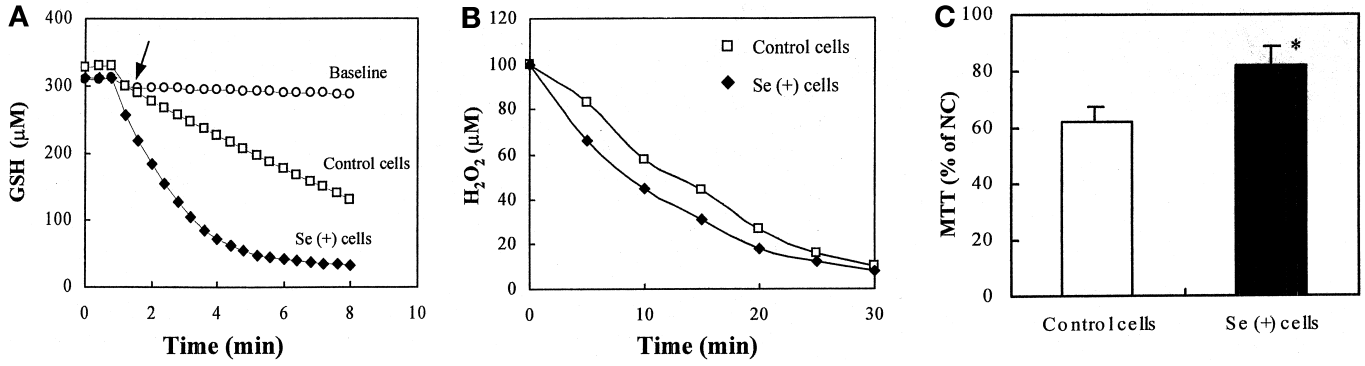

Fig. 7. The in vitro GSH depletion, H_2O_2 metabolism, and peroxide-induced cytotoxicity (MTT assay) for Se (+) cells. A: In vitro GSH depletion assay. GSH depletion was measured with cell lysates from Se (+) cells (filled diamonds) and control cells (open squares). Baseline (open circles) represents all reagents except cell lysate. One hundred micrograms of cell protein was used for each sample and details are provided in Materials and Methods. The arrow indicates the time of *t*-BuOOH (200 μM) addition. The results are representative of three experiments. B: H_2O_2 metabolism by J774A.1 macrophages. Approximately 1×10^7 J774 macrophages were plated in a 100-mm dish with 20 ml of RPMI medium. An initial concentration of 100 μM H_2O_2 was added to the medium, and 1 ml of medium was taken every 5 min to measure remaining H_2O_2 levels, using a biological oxygen monitor as described in Materials and Methods. Se (+) cells (solid diamonds); control cells (open squares). Data represent the mean of two independent experiments. C: MTT assay for peroxide-induced cytotoxicity. J774A.1 macrophages ($2–3 \times 10^5$/well in a 48-well dish) were treated with H_2O_2 (200 μM) for 30 min in PBS, followed by medium changes to 10% FBS-DMEM for an additional 24 h. Data are expressed as a percentage relative to control (NC) (n = 3). Open column, control cells; solid column, Se (+) cells. * Significantly different from control cells ($P < 0.05$).

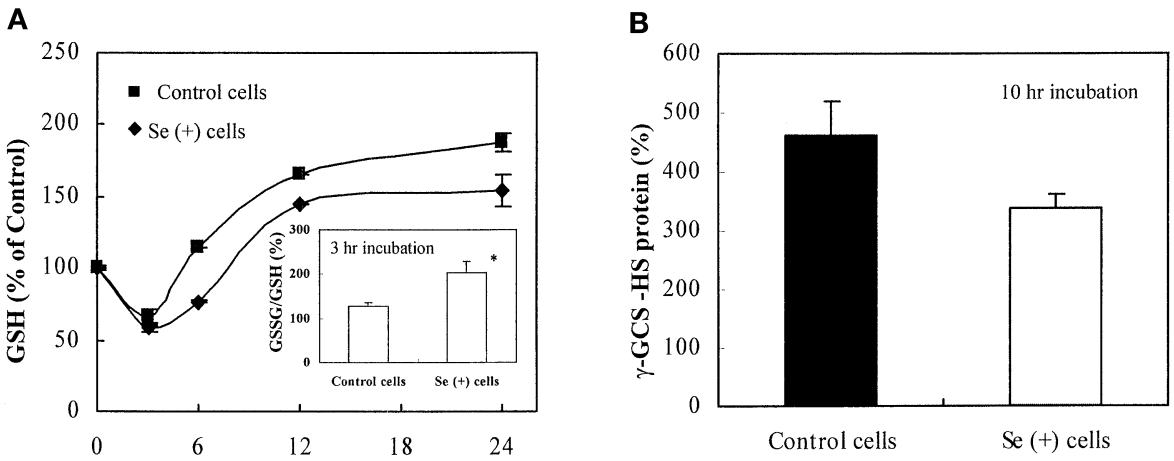

Fig. 8. Effects oxLDL on Se (+) cell GSH and γ-GCS-HS protein content. A: Se (+) cells (filled diamonds) (n = 3) and control cells (filled squares) (n = 4) (2–3 × 10^6/well) were treated with oxLDL (200 μg/ml) for up to 24 h. The GSH content is expressed as a percentage relative to control. Inset: The GSSG/GSH ratio (as a percentage of untreated control) after 3 h of oxLDL treatment. The basal ratios of GSSG/GSH were 0.04 and 0.05 in control and Se (+) cells, respectively. * $P < 0.05$ compared with control cells. Data are expressed as means ± SE (%). B: Maximum induction of γ-GCS-HS protein in Se (+) cells and control cells by oxLDL at 10 h of treatment. γ-GCS-HS protein levels were determined by Western analysis, using anti-rat γ-GCS-HS antibody. Solid column, control cells (n = 4); open column, Se (+) cells (n = 3).

DISCUSSION

The formation of oxLDL in the artery wall is thought to be a process that initiates and accelerates atherosclerotic lesion development (36). OxLDL appears to have a number of properties that include the ability to stimulate monocyte/macrophage chemotaxis, induce expression of proinflammatory cytokines, impair vasodilatation, and produce toxicity to endothelial cells (37).

OxLDL-induced oxidative stress and GSH depletion and repletion have been described in many cell types (19, 20, 38). These changes in GSH levels are not specific to the heavily oxidized LDL. LDL^- (a mildly oxidized LDL that is isolated from human plasma) shows a similar but less severe effect. However, LDL^- is recognized mostly by nLDL receptor (32), and thus the extent of LDL^- uptake and amount of peroxide delivered to macrophages is likely to be much less than oxLDL, which is taken up by high capacity scavenger receptors. Similarly, nLDL and AcLDL with low levels of oxidized lipid have little if any effect on GSH levels. These data suggest that the oxidized lipids in LDL particles are primarily responsible for depletion of cellular GSH and account substantially for the induction of GSH synthesis. The extent of GSH changes is correlated with the level of LDL lipid oxidation and the amount of LDL-associated oxidized lipid taken up by cells.

OxLDL-mediated GSH depletion is thought to be due to the activity of GPx (11) and GST (12, 39), which metabolize oxLDL-associated LOOH or aldehydes at the expense of GSH. However, GPx-mediated GSH oxidation is primarily responsible for rapid GSSG formation. Although part of the GSSG formed can be reduced back to GSH through the action of GRD (40), the rate of GSH oxidation could exceed the rate of GSSG reduction, especially when GRD is inhibited by decreased supply of reducing equivalents. The resulting increase in GSSG/GSH ratios may have at least two consequences: *1*) a shift in the thiol redox status may activate certain oxidant-responsive transcriptional elements (41, 42); and *2*) GSSG can be preferentially secreted from cells, depleting the total nonprotein thiol pool. Our findings show that an increased GSSG/GSH ratio is positively correlated with cellular GPx levels after a 3-h treatment with oxLDL (Fig. 8A), suggesting that GSSG accumulation is due to GPx-mediated reduction of peroxides. Because GSSG is actively excreted from cells (21), current methods may underestimate the amount of GSSG produced and the actual amount of GSSG formed in response to oxidative stress may have been greater than indicated. Nevertheless, the present data show that the extent of GSH depletion and synthesis induction by oxLDL is not strictly related to increase on the GSSG/GSH ratios.

Ebselen pretreatment of oxLDL essentially abolished the peroxides but not the aldehydes in oxLDL (Fig. 3A). The substrates for ebselen include not only H_2O_2 and fatty acid hydroperoxides, but also hydroperoxides of more complex lipids such as phospholipid and cholesteryl ester hydroperoxides (43). Peroxide-depleted oxLDL did not significantly affect GSH levels. Moreover, the correlation between oxLDL-associated LOOH and the extent of GSH depletion further emphasizes the role of peroxides in oxLDL-induced GSH depletion. Under similar conditions, oxLDL-associated aldehydes alone might not be sufficient to induce GSH depletion and adaptive response. 4-Hydroxynonenal (HNE) has been reported to induce depletion of GSH followed by an adaptive increase in THP-1 cell (19). Estimation of the HNE levels in oxLDL based on the content of MDA suggests that the levels of reactive aldehydes were insufficient to induce the GSH depletion by HNE as shown in previous studies. Because oxLDL-associated HNE is taken up by scavenger receptors, using pure HNE reagent may not represent the same exposure conditions as produced with oxLDL.

The intracellular GSH levels are mainly regulated by activity of rate-limiting enzyme γ-GCS (34). γ-GCS is a heterodimer consisting of a catalytic heavy subunit containing all substrate-binding sites and a regulatory subunit that modulates the affinity of heavy subunit for substrate and inhibitors. γ-GCS-HS and γ-GCS-LS are encoded by separate genes (44). The absolute amounts and ratios of each subunit vary among different normal human tissues (45). In most cases, increases in γ-GCS-HS levels have been shown to coincide with elevation of GSH levels (46), and coordinate upregulation of regulatory subunit also has been found under oxidative stress (47). However, in HeLa cells, overexpression of the γ-GCS-LS alone appears to be sufficient to increase γ-GCS activity and GSH levels (48), suggesting a role for both subunits in GSH synthesis. For rat or human γ-GCS, about 30%–70% is stabilized by an intersubunit disulfide bond as well as noncovalent bonds (49). The formation of this intersubunit disulfide bond may be regulated by cellular redox status as influenced by depletion or repletion of GSH (50). Thus, the increased oxidative status following low level peroxide challenge could induce rapid increases in net GSH levels by means of relieving feedback inhibition on γ-GCS. However, once the GSH depletion or GSSG/GSH ratio reaches a certain level, it could trigger the de novo synthesis of GSH. What this level is has not been specified and may vary among different cells. In this study an oxLDL-induced GSH adaptive increase was found to be associated with a transient increase in γ-GCS-HS protein expression that coincided with increased de novo GSH synthesis, representing a cellular protective response against oxLDL-induced oxidative stress. The decrease in γ-GCS-HS protein content at 24 h may reflect a feedback inhibition arising from the elevated GSH. The continuous increase in GSH levels up to 24 h despite an attenuation of enzyme induction could, in part, be explained by an accumulation of GSH due to an imbalance between GSH production and limited GSH degradation as catalyzed by GGT. Our findings are consistent with the article by Kirlin et al. (51), showing that a minor GSH redox change in benzyl isothiocyanate-treated HT29 cells (12 mV of oxidation for the GSH pool) was sufficient to induce γ-GCS-HS mRNA synthesis. The time course and extent of GSH changes were similar to the oxLDL-induced changes found in our study. However, detailed relationships between GSH redox change and γ-GCS induction (and their relationship to peroxide dose vs. oxLDL dose) need further evaluation and may vary among different cell types, as does the content of GSH. Also, a combination of oxidant and receptor-mediated signaling events may account for the oxLDL dose-dependent induction of γ-GCS.

AcLDL and ebselen-treated oxLDL, both of which contain low LOOH levels, induced a small to moderate increase in γ-GCS-HS protein expression that was associated with small changes in GSH levels, and neither AcLDL nor ebselen-treated oxLDL caused a significant depletion of GSH. These suggest that the extent of peroxide-dependent GSH depletion is not the only factor determining the extent of γ-GCS induction. It is possible that peroxide-mediated GSH depletion is sufficient but not essential to induce de novo GSH synthesis; however, other peroxide-mediated reactions may facilitate formation of the intersubunit disulfide bond of γ-GCS and diminish the feedback inhibition of GSH.

The rate of de novo GSH synthesis is also determined by the availability of substrates. Cysteine, the rate-limiting substrate, is taken up by cells as cystine through the Na^+-independent X_c^- system, and once inside the cell, is rapidly reduced back to cysteine. OxLDL has been reported to increase cystine transport and GSH levels in human umbilical artery smooth muscle cells (38). Peroxides such as *t*-BuOOH and H_2O_2 also show similar effects on cystine transport in human erythrocytes (52) and human umbilical vein endothelial cells (HUVEC) (53). It is, therefore, plausible that oxLDL-associated hydroperoxides could also affect cystine transport and substrate availability for de novo GSH synthesis.

The promoter region of the γ-GCS-HS gene contains binding sites for oxidative stress response elements such as nuclear factor κB, AP-1, or TRE (54). OxLDL induction of γ-GCS-HS mRNA has been shown to be mediated by the expression of c-Fos/c-Jun and activation of AP-1 (20). This induction also takes place when using hydroperoxyeicosatetraenoic acid derivatives of arachidonic acid (55). In a similar manner, LOOH from oxLDL as well as peroxides generated inside cells (either through lipid peroxidation or by H_2O_2 formation) may activate AP-1. It is plausible that oxLDL-associated LOOH induces GSH depletion or GSSG accumulation by disturbing the cellular thiol redox status and signaling AP-1 activation and translocation through the induction of stress-activated c-Jun N-terminal protein kinase (56). AP-1 binding to its TRE consensus regions and the initiation of γ-GCS gene transcription may occur because of the reduced environment in the cell nucleus provided by thioredoxin, nuclear redox protein Ref-1 (57), or the possible redistribution of GSH (58, 59).

GPx are considered major cellular antioxidant enzymes. Se (+) cells, which possess higher GPx activities, exhibited faster peroxide (H_2O_2) consumption rates. The rapid induction of cGPx as opposed to PHGPx has been well documented after selenium supplementation (60). As shown in this study, the enhanced peroxide detoxification capacity of Se (+) cells was linked to a more rapid GSH depletion and higher GSSG accumulation. It is reasonable that in Se (+) cells the rapid reduction of peroxides and greater capacity to metabolize administered or internally generated peroxides would result in lower concentrations of residual peroxides and affect the degree of oxidative signaling of γ-GCS expression.

The generation of ROS by vascular cells takes place after the binding of LDL particles to scavenger receptors such as CD36 (61) and LOX-1 (62). AcLDL, nLDL, and oxLDL have all been shown to increase macrophage CD36 mRNA and protein expression, with oxLDL causing the greatest induction (63). AcLDL and oxLDL were found to induce ROS production in J774 macrophages (Fig. 6). The content of LOOH in AcLDL was comparable to that in ebselen-treated oxLDL and much lower than that found

in oxLDL, suggesting that ROS generation via scavenger receptor-mediated signaling may also contribute to macrophage γ-GCS-HS protein induction. Indications that the γ-GCS gene can be induced by a number of stimuli that produce ROS (35, 64, 65) point to ROS as contributing factors for γ-GCS induction that is regulated by AP-1. Receptor-associated ROS formation is, however, small compared with that produced by peroxide-enriched oxLDL, which may involve numerous oxidant-sensitive responses, including GSH depletion, that induce de novo GSH synthesis.

This study was supported by grant HL50350 from the National Institutes of Health. The authors thank Hazel Peterson for help in ROS measurement.

Manuscript received 18 September 2000 and in revised form 11 January 2001.

REFERENCES

1. Berliner, J. A., and J. W. Heinecke. 1996. The role of oxidized lipoproteins in atherogenesis. *Free Radic. Biol. Med.* **20:** 707–727.
2. Garner, B., and W. Jessup. 1996. Cell-mediated oxidation of low-density lipoprotein: the elusive mechanism(s). *Redox Rep.* **2:** 97–104.
3. Rankin, S. M., S. Parthasarathy, and D. Steinberg. 1991. Evidence for a dominant role of lipoxygenase(s) in the oxidation of LDL by mouse peritoneal macrophages. *J. Lipid Res.* **32:** 449–456.
4. Aviram, M., M. Rosenblat, A. Etzioni, and R. Levy. 1996. Activation of NADPH oxidase required for macrophage-mediated oxidation of low-density lipoprotein. *Metabolism.* **45:** 1069–1079.
5. Heinecke, J. W. 1997. Pathways for oxidation of low density lipoprotein by myeloperoxidase: tyrosyl radical, reactive aldehydes, hypochlorous acid and molecular chlorine. *Biofactors.* **6:** 145–155.
6. Podrez, E. A., M. Febbraio, N. Sheibani, D. Schmitt, R. L. Silverstein, D. P. Hajjar, P. A. Cohen, W. A. Frazier, H. F. Hoff, and S. L. Hazen. 2000. Macrophage scavenger receptor CD36 is the major receptor for LDL modified by monocyte-generated reactive nitrogen species. *J. Clin. Invest.* **105:** 1095–1108.
7. Kodama, T., P. Reddy, C. Kishimoto, and M. Krieger. 1988. Purification and characterization of a bovine acetyl low density lipoprotein receptor. *Proc. Natl. Acad. Sci. USA.* **85:** 9238–9242.
8. Endemann, G., L. W. Stanton, K. S. Madden, C. M. Bryant, R. T. White, and A. A. Protter. 1993. CD36 is a receptor for oxidized low density lipoprotein. *J. Biol. Chem.* **268:** 11811–11816.
9. Dhaliwal, B. S., and U. P. Steinbrecher. 1999. Scavenger receptors and oxidized low density lipoproteins. *Clin. Chim. Acta.* **286:** 191–205.
10. Kalyanaraman, B., H. Karoui, R. J. Singh, and C. C. Felix. 1996. Detection of thiyl radical adducts formed during hydroxyl radical- and peroxynitrite-mediated oxidation of thiols—a high resolution ESR spin-trapping study at Q-band (35 GHz). *Anal. Biochem.* **241:** 75–81.
11. Ursini, F., M. Maiorino, R. Brigelius-Flohe, K. D. Aumann, A. Roveri, D. Schomburg, and L. Flohe. 1995. Diversity of glutathione peroxidases. *Methods Enzymol.* **252:** 38–53.
12. Armstrong, R. N. 1997. Structure, catalytic mechanism, and evolution of the glutathione transferases. *Chem. Res. Toxicol.* **10:** 2–18.
13. Meister, A. 1973. On the enzymology of amino acid transport. *Science.* **180:** 33–39.
14. Anderson, M. E., R. J. Bridges, and A. Meister. 1980. Direct evidence for inter-organ transport of glutathione and that the nonfiltration renal mechanism for glutathione utilization involves gamma-glutamyl transpeptidase. *Biochem. Biophys. Res. Commun.* **96:** 848–853.
15. Richman, P. G., and A. Meister. 1975. Regulation of gamma-glutamyl-cysteine synthetase by nonallosteric feedback inhibition by glutathione. *J. Biol. Chem.* **250:** 1422–1426.
16. Ochi, T. 1993. Mechanism for the changes in levels of glutathione upon exposure of cultured mammalian cells to tertiary-butylhydroperoxide and diamide. *Arch. Toxicol.* **67:** 401–410.
17. Kennedy, K. A., and N. L. Lane. 1994. Effect of in vivo hyperoxia on the glutathione system in neonatal rat lung. *Exp. Lung Res.* **20:** 73–83.
18. Purucker, E., and J. Lutz. 1992. Effect of hyperbaric oxygen treatment and perfluorochemical administration on glutathione status of the lung. *Adv. Exp. Med. Biol.* **317:** 131–136.
19. Darley-Usmar, V. M., A. Severn, V. J. O'Leary, and M. Rogers. 1991. Treatment of macrophages with oxidized low-density lipoprotein increases their intracellular glutathione content. *Biochem. J.* **278:** 429–434.
20. Cho, S., M. Hazama, Y. Urata, S. Goto, S. Horiuchi, K. Sumikawa, and T. Kondo. 1999. Protective role of glutathione synthesis in response to oxidized low density lipoprotein in human vascular endothelial cells. *Free Radic. Biol. Med.* **26:** 589–602.
21. Ishikawa, T., and H. Sies. 1984. Cardiac transport of glutathione disulfide and S-conjugate. Studies with isolated perfused rat heart during hydroperoxide metabolism. *J. Biol. Chem.* **259:** 3838–3843.
22. Angel, P., and M. Karin. 1991. The role of Jun, Fos and the AP-1 complex in cell-proliferation and transformation. *Biochim. Biophys. Acta.* **1072:** 129–157.
23. Hodis, H. N., D. M. Kramsch, P. Avogaro, G. Bittolo-Bon, G. Cazzolato, J. Hwang, H. Peterson, and A. Sevanian. 1994. Biochemical and cytotoxic characteristics of an in vivo circulating oxidized low density lipoprotein (LDL-). *J. Lipid Res.* **35:** 669–677.
24. Basu, S. K., J. L. Goldstein, G. W. Anderson, and M. S. Brown. 1976. Degradation of cationized low density lipoprotein and regulation of cholesterol metabolism in homozygous familial hypercholesterolemia fibroblasts. *Proc. Natl. Acad. Sci. USA.* **73:** 3178–3182.
25. Antunesab, F., and E. Cadenasa. 2000. Estimation of H_2O_2 gradients across biomembranes. *FEBS Lett.* **475:** 121–126.
26. Auerbach, B. J., J. S. Kiely, and J. A. Cornicelli. 1992. A spectrophotometric microtiter-based assay for the detection of hydroperoxy derivatives of linoleic acid. *Anal. Biochem.* **201:** 375–380.
27. Buege, J. A., and S. D. Aust. 1978. Microsomal lipid peroxidation. *Methods Enzymol.* **52:** 302–310.
28. Roveri, A., M. Maiorino, and F. Ursini. 1994. Enzymatic and immunological measurements of soluble and membrane-bound phospholipid-hydroperoxide glutathione peroxidase. *Methods Enzymol.* **233:** 202–212.
29. Eklow, L., P. Moldeus, and S. Orrenius. 1984. Oxidation of glutathione during hydroperoxide metabolism. A study using isolated hepatocytes and the glutathione reductase inhibitor 1,3-bis(2-chloroethyl)-1-nitrosourea. *Eur. J. Biochem.* **138:** 459–463.
30. Fariss, M. W., and D. J. Reed. 1987. High-performance liquid chromatography of thiols and disulfides: dinitrophenol derivatives. *Methods Enzymol.* **143:** 101–109.
31. Denizot, F., and R. Lang. 1986. Rapid colorimetric assay for cell growth and survival. Modifications to the tetrazolium dye procedure giving improved sensitivity and reliability. *J. Immunol. Methods.* **89:** 271–277.
32. Avogaro, P., G. B. Bon, and G. Cazzolato. 1988. Presence of a modified low density lipoprotein in humans. *Arteriosclerosis.* **8:** 79–87.
33. Sies, H. 1993. Ebselen, a selenoorganic compound as glutathione peroxidase mimic. *Free Radic. Biol. Med.* **14:** 313–323.
34. Yan, N., and A. Meister. 1990. Amino acid sequence of rat kidney gamma-glutamylcysteine synthetase. *J. Biol. Chem.* **265:** 1588–1593.
35. Rahman, I., A. Bel, B. Mulier, M. F. Lawson, D. J. Harrison, W. Macnee, and C. A. Smith. 1996. Transcriptional regulation of gamma-glutamylcysteine synthetase-heavy subunit by oxidants in human alveolar epithelial cells. *Biochem. Biophys. Res. Commun.* **229:** 832–837.
36. Steinberg, D. 1997. Low density lipoprotein oxidation and its pathobiological significance. *J. Biol. Chem.* **272:** 20963–20966.
37. Klatt, P., and H. Esterbauer. 1996. Oxidative hypothesis of atherogenesis. *J. Cardiovasc. Risk.* **3:** 346–351.
38. Siow, R. C., H. Sato, D. S. Leake, J. D. Pearson, S. Bannai, and G. E. Mann. 1998. Vitamin C protects human arterial smooth muscle cells against atherogenic lipoproteins: effects of antioxidant vitamins C and E on oxidized LDL-induced adaptive increases in cystine transport and glutathione. *Arterioscler. Thromb. Vasc. Biol.* **18:** 1662–1670.
39. Hurst, R., Y. Bao, P. Jemth, B. Mannervik, and G. Williamson. 1998. Phospholipid hydroperoxide glutathione peroxidase activity of human glutathione transferases. *Biochem. J.* **332:** 97–100.
40. Akerboom, T. P., M. Bilzer, and H. Sies. 1982. The relationship of biliary glutathione disulfide efflux and intracellular glutathione disulfide content in perfused rat liver. *J. Biol. Chem.* **257:** 4248–4252.

41. Sen, C. K., and L. Packer. 1996. Antioxidant and redox regulation of gene transcription. *FASEB J.* **10:** 709–720.
42. Muller, J. M., R. A. Rupec, and P. A. Baeuerle. 1997. Study of gene regulation by NF-kappa B and AP-1 in response to reactive oxygen intermediates. *Methods.* **11:** 301–312.
43. Sattler, W., M. Maiorino, and R. Stocker. 1994. Reduction of HDL- and LDL-associated cholesteryl ester and phospholipid hydroperoxides by phospholipid hydroperoxide glutathione peroxidase and Ebselen (PZ 51). *Arch. Biochem. Biophys.* **309:** 214–221.
44. Tsuchiya, K., R. T. Mulcahy, L. L. Reid, C. M. Disteche, and T. J. Kavanagh. 1995. Mapping of the glutamate-cysteine ligase catalytic subunit gene (GLCLC) to human chromosome 6p12 and mouse chromosome 9D-E and of the regulatory subunit gene (GLCLR) to human chromosome 1p21-p22 and mouse chromosome 3H1–3. *Genomics.* **30:** 630–632.
45. Gipp, J. J., H. H. Bailey, and R. T. Mulcahy. 1995. Cloning and sequencing of the cDNA for the light subunit of human liver gamma-glutamylcysteine synthetase and relative mRNA levels for heavy and light subunits in human normal tissues. *Biochem. Biophys. Res. Commun.* **206:** 584–589.
46. Mulcahy, R. T., H. H. Bailey, and J. J. Gipp. 1994. Up-regulation of gamma-glutamylcysteine synthetase activity in melphalan-resistant human multiple myeloma cells expressing increased glutathione levels. *Cancer Chemother. Pharmacol.* **34:** 67–71.
47. Galloway, D. C., D. G. Blake, A. G. Shepherd, and L. I. McLellan. 1997. Regulation of human gamma-glutamylcysteine synthetase: co-ordinate induction of the catalytic and regulatory subunits in HepG2 cells. *Biochem. J.* **328:** 99–104.
48. Tipnis, S. R., D. G. Blake, A. G. Shepherd, and L. I. McLellan. 1999. Overexpression of the regulatory subunit of gamma-glutamylcysteine synthetase in HeLa cells increases gamma-glutamylcysteine synthetase activity and confers drug resistance. *Biochem. J.* **337:** 559–566.
49. Seelig, G. F., R. P. Simondsen, and A. Meister. 1984. Reversible dissociation of gamma-glutamylcysteine synthetase into two subunits. *J. Biol. Chem.* **259:** 9345–9347.
50. Huang, C. S., L. S. Chang, M. E. Anderson, and A. Meister. 1993. Catalytic and regulatory properties of the heavy subunit of rat kidney gamma-glutamylcysteine synthetase. *J. Biol. Chem.* **268:** 19675–19680.
51. Kirlin, W. G., J. Cai, S. A. Thompson, D. Diaz, T. J. Kavanagh, and D. P. Jones. 1999. Glutathione redox potential in response to differentiation and enzyme inducers. *Free Radic. Biol. Med.* **27:** 1208–1218.
52. Ohtsuka, Y., T. Kondo, and Y. Kawakami. 1988. Oxidative stresses induced the cystine transport activity in human erythrocytes. *Biochem. Biophys. Res. Commun.* **155:** 160–166.
53. Miura, K., T. Ishii, Y. Sugita, and S. Bannai. 1992. Cystine uptake and glutathione level in endothelial cells exposed to oxidative stress. *Am. J. Physiol.* **262:** C50–C58.
54. Mulcahy, R. T., M. A. Wartman, H. H. Bailey, and J. J. Gipp. 1997. Constitutive and beta-naphthoflavone-induced expression of the human gamma-glutamylcysteine synthetase heavy subunit gene is regulated by a distal antioxidant response element/TRE sequence. *J. Biol. Chem.* **272:** 7445–7454.
55. Rao, G. N., W. C. Glasgow, T. E. Eling, and M. S. Runge. 1996. Role of hydroperoxyeicosatetraenoic acids in oxidative stress-induced activating protein 1 (AP-1) activity. *J. Biol. Chem.* **271:** 27760–27764.
56. Wilhelm, D., K. Bender, A. Knebel, and P. Angel. 1997. The level of intracellular glutathione is a key regulator for the induction of stress-activated signal transduction pathways including Jun N-terminal protein kinases and p38 kinase by alkylating agents. *Mol. Cell. Biol.* **17:** 4792–4800.
57. Hirota, K., M. Matsui, S. Iwata, A. Nishiyama, K. Mori, and J. Yodoi. 1997. AP-1 transcriptional activity is regulated by a direct association between thioredoxin and Ref-1. *Proc. Natl. Acad. Sci. USA.* **94:** 3633–3638.
58. Briviba, K., G. Fraser, H. Sies, and B. Ketterer. 1993. Distribution of the monochlorobimane-glutathione conjugate between nucleus and cytosol in isolated hepatocytes. *Biochem. J.* **294:** 631–633.
59. Voehringer, D. W., D. J. McConkey, T. J. McDonnell, S. Brisbay, and R. E. Meyn. 1998. Bcl-2 expression causes redistribution of glutathione to the nucleus. *Proc. Natl. Acad. Sci. USA.* **95:** 2956–2960.
60. Brigelius-Flohe, R. 1999. Tissue-specific functions of individual glutathione peroxidases. *Free Radic. Biol. Med.* **27:** 951–965.
61. Maxeiner, H., J. Husemann, C. A. Thomas, J. D. Loike, J. El Khoury, and S. C. Silverstein. 1998. Complementary roles for scavenger receptor A and CD36 of human monocyte-derived macrophages in adhesion to surfaces coated with oxidized low-density lipoproteins and in secretion of H_2O_2. *J. Exp. Med.* **188:** 2257–2265.
62. Cominacini, L., A. F. Pasini, U. Garbin, A. Davoli, M. L. Tosetti, M. Campagnola, A. Rigoni, A. M. Pastorino, V. LoCascio, and T. Sawamura. 2000. Oxidized low density lipoprotein (ox-LDL) binding to ox-LDL receptor-1 in endothelial cells induces the activation of NF-kappaB through an increased production of intracellular reactive oxygen species. *J. Biol. Chem.* **275:** 12633–12638.
63. Han, J., D. P. Hajjar, M. Febbraio, and A. C. Nicholson. 1997. Native and modified low density lipoproteins increase the functional expression of the macrophage class B scavenger receptor, CD36. *J. Biol. Chem.* **272:** 21654–21659.
64. Tian, L., M. M. Shi, and H. J. Forman. 1997. Increased transcription of the regulatory subunit of gamma-glutamylcysteine synthetase in rat lung epithelial L2 cells exposed to oxidative stress or glutathione depletion. *Arch. Biochem. Biophys.* **342:** 126–133.
65. Shi, M. M., A. Kugelman, T. Iwamoto, L. Tian, and H. J. Forman. 1994. Quinone-induced oxidative stress elevates glutathione and induces gamma-glutamylcysteine synthetase activity in rat lung epithelial L2 cells. *J. Biol. Chem.* **269:** 26512–26517.